Journal of Organometallic Chemistry, 228 (1982) 309—320
Elsevier Sequoia S.A., Lausanne — Printed in The Netherlands

THEORETICAL COMPARISON OF THE "SLIP" DISTORTION AND ROTATIONAL BARRIERS IN COMPARABLE SEVEN AND TWELVE VERTEX CARBAPLATINABORANES

MARIA J. CALHORDA and D. MICHAEL P. MINGOS *
Inorganic Chemistry Laboratory, University of Oxford, South Parks Road, Oxford OX1 3QR (Great Britain)

and ALAN J. WELCH
Department of Chemistry, City University, London EC1V OHB (Great Britain)

(Received October 13th, 1981)

Summary

Extended Hückel molecular orbital calculations on the related *closo*-platinaboranes $[(H_3P)_2Pt(B_{11}H_{11})]^{2-}$ and $[(H_3P)_2Pt(B_6H_6)]^{2-}$ and the *closo*-carbaplatinaboranes $[(H_3P)_2Pt(C_2B_9H_{11})]$ and $[(H_3P)_2Pt(C_2B_4H_6)]$ have suggested that the larger "slip" distortions in the pentagonal bipyramidal derivatives can be attributed in large measure to the different metal—ligand interactions which are induced by the different elevation angles of the substituents on the pentagonal faces of the ligands. Differences in bond lengths associated with the two classes of carbaplatinaboranes have been interpreted in terms of the different bonding capabilities of the two types of carbaborane ligands.

The "slip" distortion in electron rich carbametalloboranes was first recognized more than a decade ago as a result of an extensive investigation of sandwich complexes derived from the carbaborane ligand $1,2\text{-}C_2B_9H_{11}{}^{2-}$ by Hawthorne and his coworkers [1]. Following several qualitative attempts at rationalising this phenomenon [2—6] we reported in 1978 extended Hückel molecular orbital calculations on these sandwich complexes which satisfactorily accounted for the extent and direction of the observed "slip" distortion [7]. X-ray crystallographic studies on the related icosahedral carbametallaboranes $[1,1\text{-}(PhMe_2P)_2\text{-}2,4\text{-}Me_2\text{-}1,2,4\text{-}PtC_2B_9H_9]$ (1), $[2,2\text{-}(Bu^tNC)_2\text{-}1\text{-}Me_3N\text{-}2,1\text{-}PdCB_{10}H_{10}]$ (2) and $[3,3\text{-}(Et_3P)_2\text{-}3,2,1\text{-}PtC_2B_9H_{11}]$ (3) by Welch et al. [8—10] clearly established that the orientations and "slip" distortions of the angular ML_2 group (both defined with respect to the polyhedron) in these complexes are highly selective. Subsequent molecular orbital calculations demonstrated that the number and positions of the carbon atoms in the metalla-bonded polyhedral face are

0022-328X/82/0000—0000/$02.75

largely responsible for these structural features [11,12].

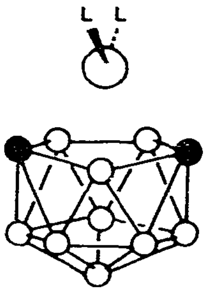

(1)

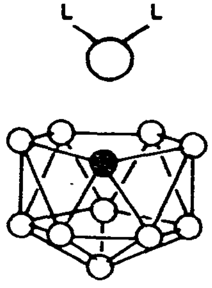

(2)

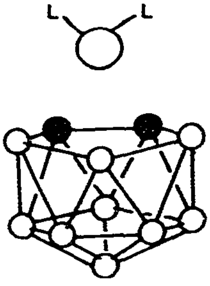

(3)

More recently the synthesis and structural characterisation of the compounds [1,1-$(Et_3P)_2$-2,3-Me_2-1,2,3-$PtC_2B_4H_4$] (4) and [1,1-$(Et_3P)_2$-1,2,4-$PtC_2B_4H_6$] (5), two isomers of the seven vertex carbaplatinaborane [$Pt(PEt_3)_2(R_2C_2B_4H_4)$] whose polyhedral skeletons differ only in respect to the position of the cage carbon atoms, have been reported [13]. These *closo*- seven vertex carbametallaboranes are structurally based on the pentagonal bipyramid with the metal atom occupying one of the apical sites. Thus these seven vertex compounds are directly comparable to the 12 vertex carbametallaboranes 1, 2 and 3. However, close comparisons of the relevant structural parameters have revealed the following differences in molecular parameters.

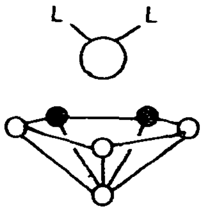

(4)

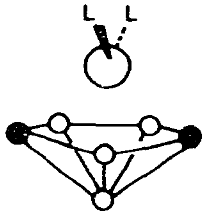

(5)

The pentagonal rings of the seven atom species are generally smaller than those of related icosahedral molecules, although the distances to their respective capping atoms (either metal or boron) are maintained. These reductions in observed atomic radii are even greater for links involving carbon. Thus a typical B—B separation of ca. 1.77 Å drops to ca. 1.71 Å (3% reduction) in the equatorial belt of the pentagonal bipyramid, whilst B—C falls from ca. 1.71 to 1.57 Å (8% reduction) and C—C is reduced from ca. 1.61 to only 1.46 Å (9% reduction). Given that the distances in the carbaborane face, which is bonded to the metal atom, are smaller as one moves from the 12 to the 7 vertex system, retention of identical M—B distances requires the metal atom to move farther from the coordinated face in the seven vertex polyhedra.

The elevation angles of substituents terminally bound to the coordinated faces of the ligands are quite different in the two classes of carbametallaboranes. In the pentagonal bipyramid the substituents are essentially coplanar with the ring, whereas in the icosahedron they are displaced towards the metal and define an elevation angle θ of ca. 26° with respect to the coordinated pentagonal face of the ligand.

Comparison of the structural data for 1 and 5 has established that although the Pt—B bond lengths are maintained on passing from the icosahedron to the pentagonal bipyramid the corresponding Pt—C distances are significantly longer in the icosahedral molecule. Furthermore, the observation of two crystallographically independent molecules in the asymmetric unit of 5 with different $Pt(PEt_3)_2$-cage conformations suggested that the rotational barriers for $Pt(PEt_3)_2$ rotation may be smaller in the pentagonal bipyramidal than the icosahedral molecules. This has been confirmed by variable temperature NMR studies on 5 [13].

The "slip" distortion in the pentagonal bipyramidal complex 4 appears to be substantially larger than that observed in the corresponding icosahedral molecule 3 on the basis of the substantially longer Pt—C distances, shorter Pt—B distances and the larger folding distortion in the former.

These subtle structural differences provide an interesting challenge for the general bonding model which we have developed to account for the conformational preferences and "slip" distortions in icosahedral carbaplatinaboranes [11,12]. Of course the extended Hückel method used for such calculations is an approximate one with many deficiencies; nonetheless the semi-quantitative conclusions derived from such calculations have been shown to have wide validity if care is taken to extract the important symmetry and perturbation theory aspects of the problem [14].

Calculations

All calculations were made using the extended Hückel method. The basis set for the platinum atom consisted of the 5*d*, 6*s* and 6*p* orbitals. The *s* and *p* orbitals were described by single Slater type wavefunctions and the *d* orbital wave functions were taken as contracted linear combinations of two Slater type wave functions. The orbital exponents were those suggested by Basch and Gray [15]. The parameters for the extended Hückel calculations are summarised below:

Orbital		Slater Exponent	H_{ii} (eV)	Ref.
H	1*s*	1.300	—13.60	16
B	2*s*	1.300	—15.20	16
	2*p*	1.300	—8.50	16
P	3*s*	1.600	—18.60	16
	3*p*	1.600	—14.00	16
C	2*s*	1.625	—21.40	16
	2*p*	1.625	—11.40	16
Pt	6*s*	2.554	—9.80	17
	6*p*	2.554	—5.35	17

Pt *d* wavefunctions:

Orbital	H_{ii}	ζ_1	c_1	ζ_2	c_2	ref
Pt 5*d*	—10.61	6.013	0.633	2.696	0.551	17

(1 eV = 96.5 kJ mol^{-1})

The calculations were made on the ICL 2900 computer at the Oxford University Computer Centre using the ICON8 program developed by Hoffmann and coworkers at Cornell University [16,18]. The calculations were made on the model pentagonal bipyramidal compounds $[Pt(PH_3)_2(B_6H_6)]^{2-}$ and $[Pt(PH_3)_2(C_2B_4H_6)]$. The borane and carbaborane fragments were idealised as *nido*-C_{5v} fragments with dimensions B—B = B—C = 1.600 Å, $B_{equatorial}$—B_{axial} = 1.770 Å. The former bond length was chosen on the basis of the average equatorial bond length in compound 5. These bond lengths were also varied in the manner discussed in some detail in the text. The B—H and C—H bond lengths were set equal to 1.200 Å. The platinum atom which completes the polyhedron was constrained initially to lie along the five fold axis with Pt—C = Pt—B = 2.470 Å. The slip distortions in these complexes were defined in terms of a lateral displacement of the platinum relative to the plane defined by the five adjacent boron atoms in the manner defined previously. The geometries of the phosphine ligands were idealised and the parameters P—H = 1.420 Å and Pt—P—H = 109.47° were used. The platinum-phosphine moiety was constrained to have C_{2v} symmetry with a P—Pt—P angle of 105° and a Pt—P bond length of 2.300 Å [13].

The molecular dimensions of the icosahedral molecules $[Pt(B_{11}H_{11})(PH_3)_2]^{2-}$ and $[Pt(C_2B_9H_{11})(PH_3)_2]$ were identical with those described previously [11].

Results and discussion

The analysis of the bonding in the seven and twelve vertex carbametallaboranes follows that described in previous papers [11,12]. Initially the bonding in the higher symmetry species $[Pt(PH_3)_2(B_6H_6)]^{2-}$ (6) and $[Pt(PH_3)_2(B_{11}H_{11})]^{2-}$ (7) are evaluated and then the effect of carbon substituents into the borane polyhedral fragment are considered as a perturbation on the general model.

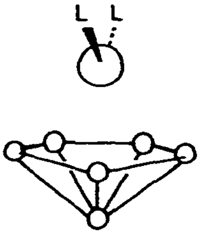

(6)

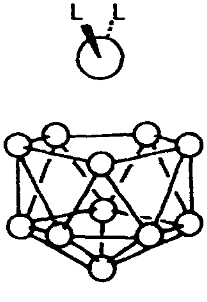

(7)

Figure 1 illustrates the relevant interaction diagrams for 6 and 7 in terms of the $Pt(PH_3)_2$ and *nido*-$B_6H_6^{2-}$ and $B_{11}H_{11}^{2-}$ fragments. The bonding capabilities of $Pt(PH_3)_2$ have been discussed in some detail previously by ourselves and other workers and therefore will not be recounted here. The frontier molecular orbitals of the *nido*-$B_6H_6^{2-}$ and $B_{11}H_{11}^{2-}$ comprise in order of increasing stability $e_2(\pi)$, $e_1(\pi)$, $e_2(\sigma)$ and $a_1(\pi)$, with the highest occupied orbital in each case being $e_1(\pi)$, which is occupied by two electrons. The $e_2(\pi)$, $e_1(\pi)$ and $a_1(\pi)$ molecular orbitals of $B_6H_6^{2-}$ and $B_{11}H_{11}^{2-}$ bear a remarkable similarity to the π-molecular

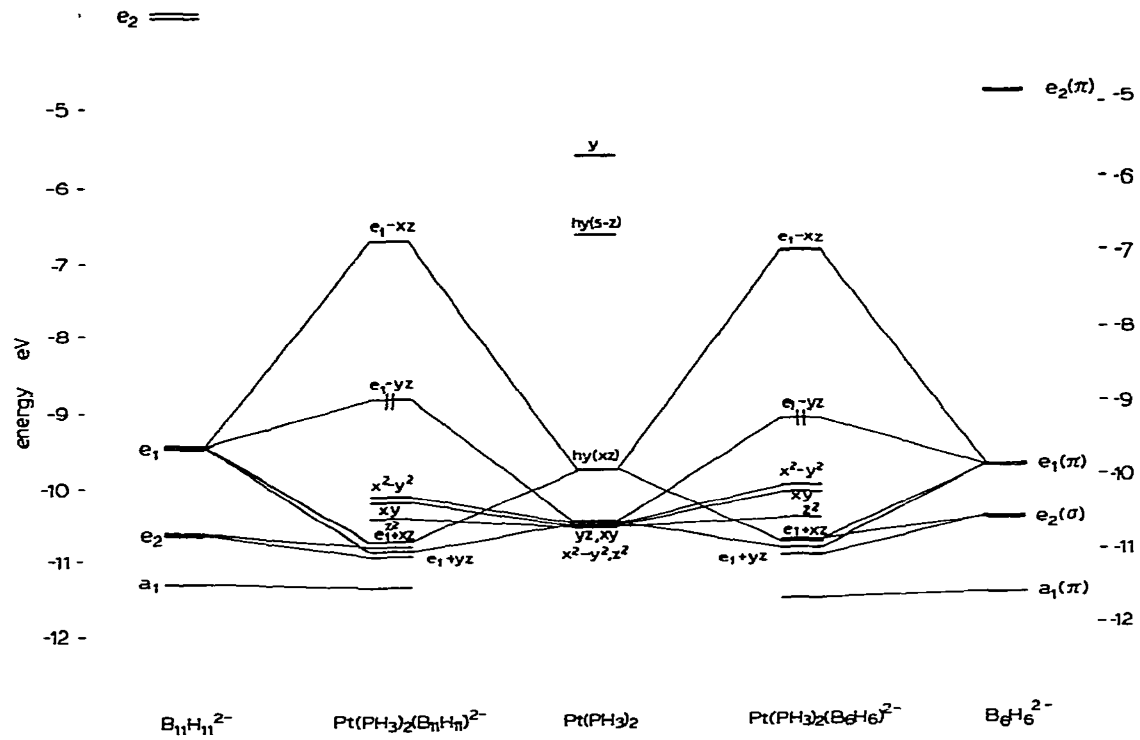

Fig. 1. Molecular orbital interaction diagrams for the complexes $[Pt(PH_3)_2(B_6H_6)]^{2-}$ (6) and $[Pt(PH_3)_2(B_{11}H_{11})]^{2-}$ (7). Particularly striking is the close similarity in the energies of the frontier molecular orbitals of the fragments and complexes.

TABLE 1

COMPUTED INTERFRAGMENT OVERLAP INTEGRALS AND OVERLAP POPULATIONS FOR $Pt(PH_3)_2(B_6H_6)^{2-}$ AND $Pt(PH_3)_2(B_{11}H_{11})^{2-}$

Overlap integrals	Orbital	Energy (eV)	$hy(xz)$	y	$hy(s{-}p_z)$	yz
$B_6H_6^{2-}$						
	$e_1(\pi)$	−9.85	0.285	0.382		0.154
	$a_1(\pi)$	−11.59			0.477	
$B_{11}H_{11}^{2-}$	$e_1(\pi)$	−9.50	0.293	0.366		0.168
($\theta = 26°$)	$a_1(\pi)$	−11.31			0.434	
$B_{11}H_{11}^{2-}$	$e_1(\pi)$	−9.79	0.262	0.345		0.137
($\theta = 0°$)	$a_1(\pi)$	−11.11			0.313	
Overlap populations						
$B_6H_6^{2-}$	$e_1(\pi)$		0.438	0.326		−0.019
	$a_1(\pi)$				0.416	
$B_{11}H_{11}^{2-}$	$e_1(\pi)$		0.452	0.355		−0.028
($\theta = 26°$)	$a_1(\pi)$				0.323	
$B_{11}H_{11}^{2-}$	$e_1(\pi)$		0.390	0.293		−0.013
($\theta = 0°$)	$a_1(\pi)$				0.238	

orbitals of the cyclopentadienyl anion, as noted previously [11]. This similarity is particularly striking for the pentagonal bipyramidal fragment since the molecular orbitals have a very high contribution from those boron $2p$ orbitals which are orthogonal to the B_5 plane. On moving from the pentagonal bipyramidal fragment to the icosahedral fragment the energies of these molecular orbitals remain essentially unchanged (see Table 1) but the composition of the orbitals changes as a result of the displacement of the substituents attached to the open pentagonal face of the ligand. In $B_6H_6^{2-}$ the hydrogen atoms lie in the B_5 plane and effectively point towards the origin of the parent pentagonal bipyramid. In order for the hydrogens in $B_{11}H_{11}^{2-}$ to point towards the origin of the parent icosahedron and thereby maintain the maximal B—B radical and tangential bonding interactions it is necessary for them to lie above the open pentagonal B_5 face. In practice the hydrogen substituents define an elevation angle of approximately 26° with respect to the open pentagonal face. The energetic preference for the geometry with an elevation angle of 26° is emphasized by extended Hückel calculations which have shown that the increase in elevation angle from 0—26° results in a stabilisation of nearly 2 eV. A direct consequence of this elevation angle is a rehybridisation of the $e_2(\pi)$, $e_1(\pi)$ and $a_1(\pi)$ orbitals in $B_{11}H_{11}^{2-}$ in such a way that the relevant orbitals tilt inwards and point towards the missing vertex of the icosahedron. This rehybridisation phenomenon is represented schematically in 8, and is particularly important in understanding the differences in the structural parameters for related pentagonal bipyramidal and icosahedral carbametallaboranes. Both $B_6H_6^{2-}$ and $B_{11}H_{11}^{2-}$ have a degenerate set of orbitals, $e_2(\sigma)$ in Fig. 1, located between the $e_1(\pi)$ and $a_1(\pi)$ molecular orbitals in energy terms, and which are essentially localised within the open faces of the ligands and consequently do not interact strongly with the frontier orbitals of the $Pt(PH_3)_2$ fragment (see reference 11 for an illustration of these molecular orbitals).

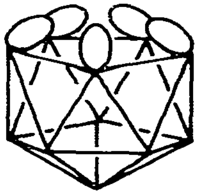

(8)

The principle bonding interactions between $Pt(PH_3)_2$ and $B_nH_n^{2-}$ fragments are indicated in Fig. 1, and their relative importance may be gauged by the Mulliken inter-fragment overlap populations summarised in Table 1. The important bonding interaction between $hy(xz)$, p_y and $hy(s—p_z)$ and the ligand $e_1(\pi)$ and $a_1(\pi)$ molecular orbitals have been discussed previously in the context of the bonding in $[Pt(PH_3)_2(B_{11}H_{11})]^{2-}$. The four electron destabilising interaction between yz and $e_1(\pi)$, which is so important in the context of the "slip" distortion observed in the related carbametallaboranes is also indicated in the Figure and confirmed by the small overlap populations in Table 1.

In order to make a meaningful comparison of the relative bonding capabilities of $B_6H_6^{2-}$ and $B_{11}H_{11}^{2-}$ with the $Pt(PH_3)_2$ fragment molecular orbital calculations on $[Pt(PH_3)_2(B_6H_6)]^{2-}$ and $[Pt(PH_3)_2(B_{11}H_{11})]^{2-}$ with identical B—B and B—Pt bond lengths (1.75 and 2.25 Å respectively) were performed initially. The overlap populations in Table 1 emphasise the close similarity in the metal cage bonding for the pentagonal and icosahedral cage compounds, when they are constrained to have equal B—B and B—Pt bond lengths. Table 1 does indicate an apparent difference in the overlap populations involving the $hy(s{-}p_z)$ molecular orbital of the $Pt(PH_3)_2$ fragment and the ligand $a_1(\pi)$ molecular orbitals. However, for the icosahedral cluster there is a lower lying cage orbital of a_1 symmetry which also contributes an interfragment overlap population of approximately the same magnitude as the deficiency noted in the Table for the icosahedron relative to the pentagonal bipyramid.

Reduction of the elevation angle from 26° to 0° in the icosahedral metallaborane causes a significant decrease in all the important interfragment overlap populations (see Table 1) and consequently results in a decrease in metal-cage bonding. Consequently the total energy decreases as the elevation angle is reduced. The extended Hückel calculations have indicated an equilibrium elevation angle of 22° for $[Pt(PH_3)_2(B_{11}H_{11})]^{2-}$ in good agreement with experimentally determined values [8—10]. In summary, the bonding requirements of the cage and their metal—ligand interactions are maximised for large elevation angles. The latter because the favourable rehybridisation of the p orbitals on the cage face illustrated in 8 lead to the larger metal—cage overlap integrals noted in Table 1.

The boron—boron overlap populations for the pentagonal bipyramidal and icosahedral platinaborane anions are illustrated in 9 and 10 and suggest that the boron—boron bonding in the equatorial pentagonal plane is stronger in the former than the latter. This reflects differences in B—B bonding in the isolated cage anions rather than the relative magnitudes of the metal—ligand bonding in the two polyhedral molecules. For the isolated $B_6H_6^{4-}$ anion the calculated overlap population of 0.923 is considerably larger than that for $B_{11}H_{11}^{4-}$ (0.712). Consequently these calculations suggest that the equatorial B—B bond lengths in the coordinated faces of the two platinaborane cages should be shorter in the case of the pentagonal bipyramid. This rationalises the contraction of the equatorial B—B and B—C distances noted in the introduction.

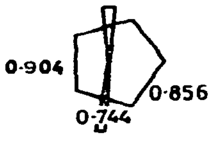

(9)

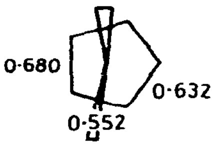

(10)

The overlap populations illustrated in 9 and 10 show the same bond alternation effects noted previously for cyclo-polyene and borane ML_2 complexes and are a direct consequence of the different bonding interactions of the $hy(xz)$ and yz orbitals of the ML_2 fragment [11].

These effects are reproduced in calculations on the more realistic carbaplatinaborane compounds $[(H_3P)_2Pt(C_2B_9H_{11})]$ and $[(H_3P)_2Pt(C_2B_4H_6)]$. The computed overlap populations for these molecules are summarised in Fig. 2. Particularly noteworthy are the stronger bonding interactions in the equatorial plane for the pentagonal bipyramidal cluster and the similarity in the metal—ligand atom overlap populations. These reproduce well the contraction in B—B and B—C distances in going from the icosahedral to the pentagonal bipyramidal polyhedron and the near constancy in the metal cage distances noted in the introduction.

The overlap populations summarised in Fig. 2 refer to calculations on the carbaplatinaboranes with the symmetrical C_s conformations illustrated in 1 and 5. However, an X-ray crystallographic analysis of $[1,1\text{-}(Et_3P)_2\text{-}1,2,4\text{-}PtC_2B_4H_6]$ (5) has revealed the presence of two crystallographically independent molecules in the asymmetric unit. One molecule has the symmetrical C_s conformation (5) and the second is a rotamer which arises by a rotation of $4\pi/5$ of the cage relative to the PtL_2 fragment. The metal cage bond lengths reflect this asymmetry and it was of interest to establish whether these effects could be reproduced

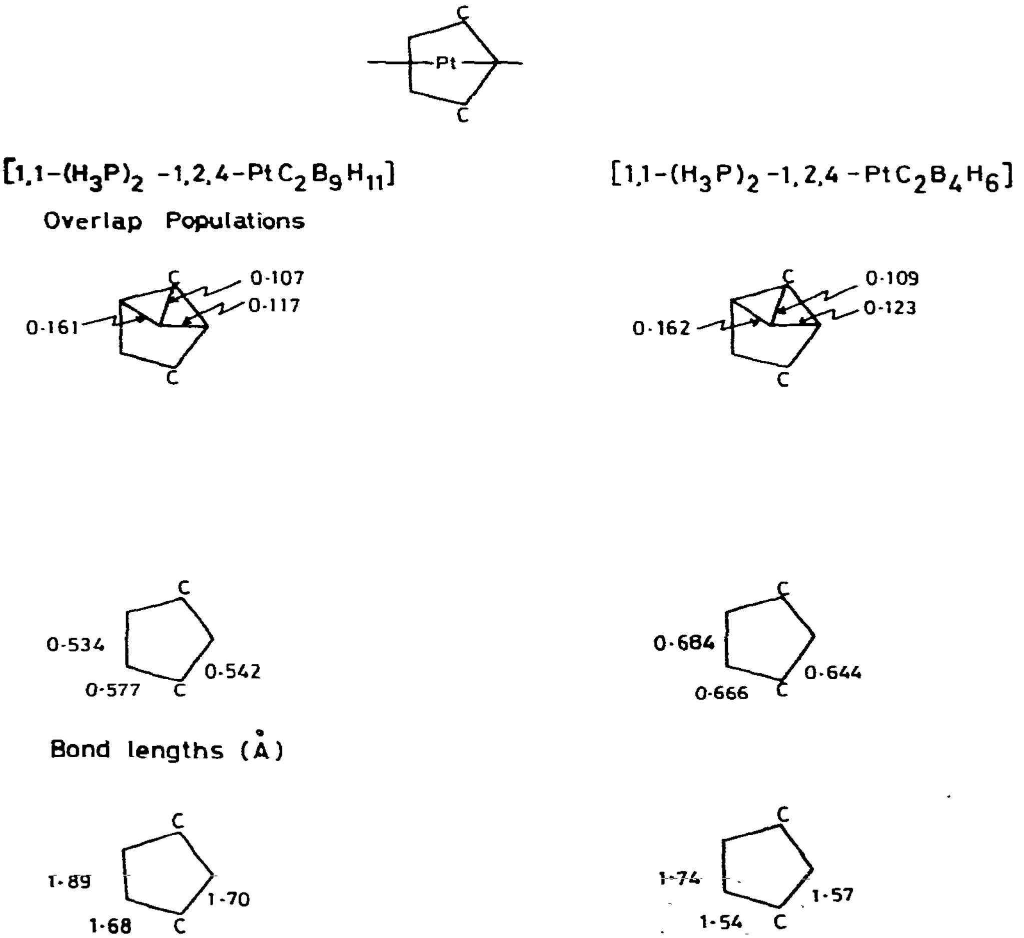

Fig. 2. Comparison of the Pt—C, Pt—B, B—B and B—C overlap populations for $[1,1\text{-}(H_3P)_2\text{-}1,2,4\text{-}PtC_2B_9H_{11}]$ and $[1,1\text{-}(H_3P)_2\text{-}1,2,4\text{-}PtC_2B_4H_6]$. A comparison of the relevant B—B and B—C bond lengths in 5 and 1 is also given at the bottom of the figure.

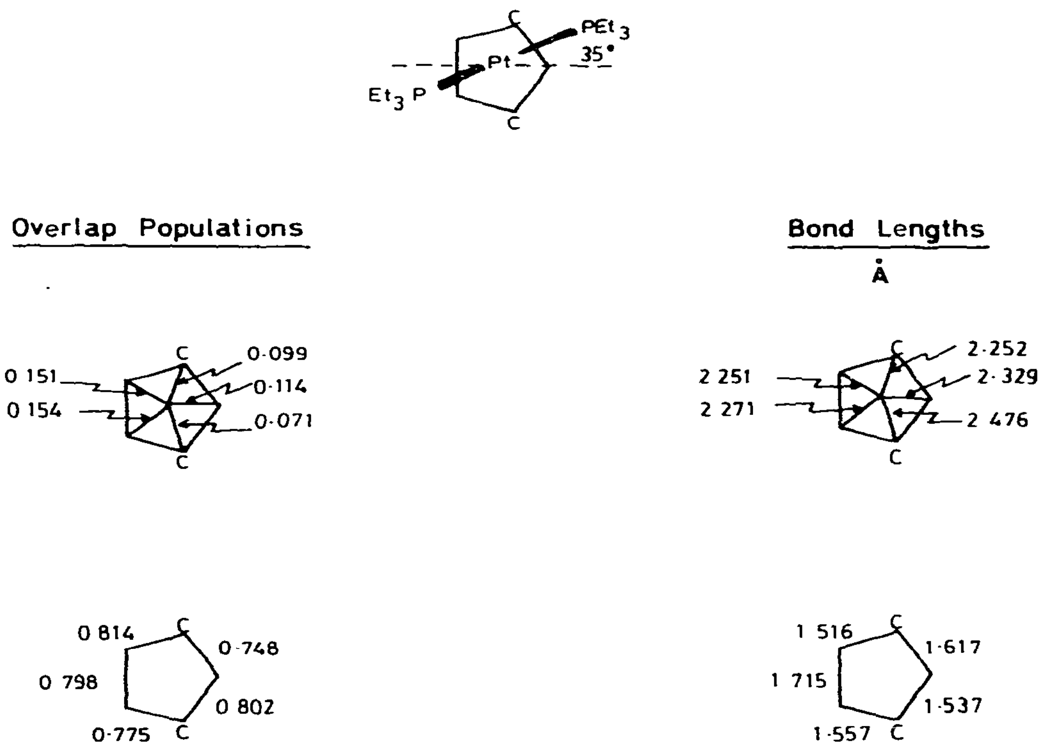

Fig. 3. Computed overlap populations for [1,1-$(H_3P)_2$-1,2,4-$PtC_2B_4H_6$] with the conformation illustrated at the top of the Figure and the experimentally determined bond lengths for the corresponding rotamer in [1,1-$(Et_3P)_2$-1,2,4-$PtC_2B_4H_6$] (taken from ref. 3).

in the extended Hückel calculations. The computed overlap populations for this second conformation are illustrated in Fig. 3 together with the observed bond lengths. The calculations do indeed reproduce the asymmetric bonding effects well.

Taking note of the contraction of the boron radii in the pentagonal bipyramid, subsequent calculations were performed for [$Pt(PH_3)_2(B_{11}H_{11})$] with a B—B bond length of 1.60 Å, i.e. the average experimentally determined equatorial bond length in 5. The Pt—B bond length was maintained at 2.25 Å in order to be consistent with the structural data on such complexes. The concommitant cage contraction and maintenance of the Pt—B bond length requires a displacement of the platinum atom away from the cage face from 1.687 to 1.792 Å.

With the appropriate geometric parameters the rotational barriers in [$Pt(PH_3)_2(C_2B_4H_6)$] and [$Pt(PH_3)_2(C_2B_9H_{11})$] were computed for a rigid rotation of the ML_2 fragment relative to coordinated pentagonal faces of the ligands. The computed rotational barrier in the case of the pentagonal bipyramidal cage compound (0.60 eV) was found to be slightly larger than that in the corresponding icosahedral carbaplatinaborane (0.47 eV), in disagreement with the experimental observations on these types of compound [13]. This discrepancy is not surprising since our estimation of the rotational barriers depends on a rigid rotor model for the PtL_2 unit above the cage and does not take into account the complexity of the rotation process and the changes in bond length either at

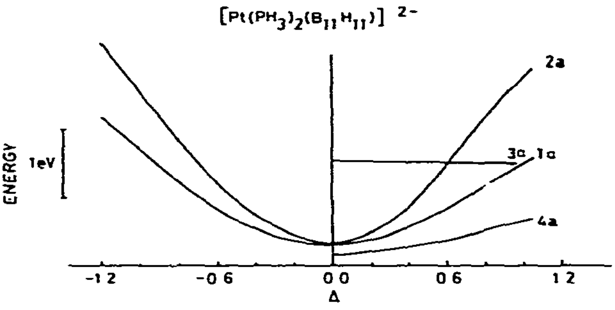

	Compound	Conformation	Substituent Elevation Angle
1a	$[Pt(PH_3)_2(B_{11}H_{11})]^{2-}$	⊥ (11)	26°
2a	$[Pt(PH_3)_2(B_{11}H_{11})]^{2-}$	// (12)	26°
3a	$[Pt(PH_3)_2(B_{11}H_{11})]^{2-}$	⊥ (11)	0°
4a	$[Pt(PH_3)_2(C_2B_9H_{11})]$	⊥ (11)	26°

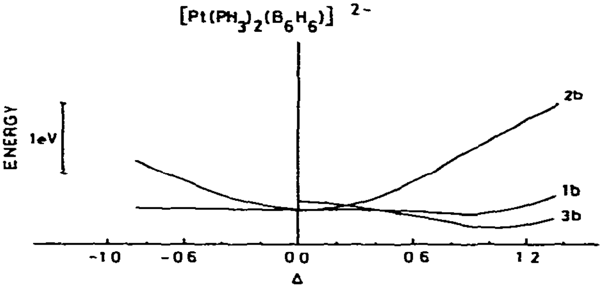

	Compound	Conformation	Substituent Elevation Angle
1b	$[Pt(PH_3)_2(B_6H_6)]^{2-}$	⊥ (11)	0°
2b	$[Pt(PH_3)_2(B_6H_6)]^{2-}$	// (12)	0°
3b	$[Pt(PH_3)_2(C_2B_4H_6)]^{2-}$	⊥ (11)	0°

Fig. 4. Effect of the "slip" distortion illustrated in 11 on the sum of the one electron energies in comparable 7 and 12 vertex platinaboranes and carbaplatinaboranes.

the energy minima or throughout the rotation process. However, our results indicate that the differences in the rotational barriers do not originate solely from the different displacements of the platinum atoms above the pentagonal faces of the ligands as previously suggested [13].

Figure 4 illustrates the potential energy surfaces for the "slip" distortions illustrated in 11 and 12 for related pentagonal and icosahedral platinaboranes with the appropriate B—B and Pt—B distances. The "slip" distortion for the parallel conformation 12 is highly unfavourable for both the pentagonal bipyramidal and icosahedral platinaboranes and the reason for this have been discussed by us previously in some detail [12]. For the perpendicular conformation 11 the "slip" distortions are more favourable.

Particularly noteworthy in the context of the present research is the energetically more favourable "slip" distortion for the pentagonal bipyramidal cage. A major contribution to this difference arises from the larger elevation angle of the substituents in the case of the icosahedral molecule, since if the calculations are repeated with a 0° elevation angle for the icosahedral cage, then it is found

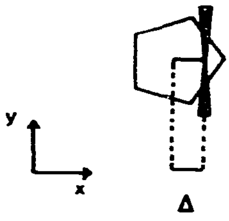

(11)

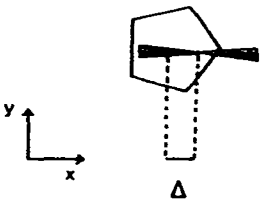

(12)

that the potential energy surfaces for the pentagonal bipyramidal and icosahedral cages are extremely similar (compare curves 3a and 1b in Fig. 4). The influence of the elevation angle on the potential energy surface for the "slip" distortion can be understood simply in term of the rehybridisation effect discussed above and illustrated in 8. If the boron *p* orbitals on the open pentagonal face of the ligand are in-pointing then they are less able to overlap effectively with the metal *d* orbitals when the metal is displaced from its central position and towards the unique boron atom (see 13).

Figure 4 also illustrates the effect of 1,2 carbon substitution on the potential energy surface for the slip distortion illustrated in 11. For both the icosahedral and pentagonal bipyramidal cage compounds the distortion becomes more favourable. The introduction of electronegative substituents at the 1,2 positions stabilise the "slip" distortion by effectively withdrawing the negative charge which accumulates at the boron atoms farthest from the metal. This effect has been discussed previously by us [12]. It is noteworthy that the potential energy surface is still more favourable for the smaller cage compound.

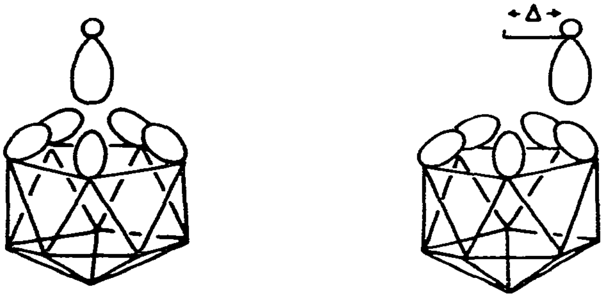

(13)

If the B—B bond lengths are reduced but the displacement of the metal atom above the pentagonal face of the $B_6H_6^{2-}$ ligand is kept constant, then the potential energy surface for the slip distortion becomes less favourable. However, when the displacement of the metal atom is increased whilst the B—B bond lengths are held constant, then the "slip" distortion becomes more favourable. Both of these effects can be simply understood in terms of the effects of these dimensional changes on the absolute magnitudes of the interfragment overlap integrals for the "slipped" and symmetrical sandwich structures. For example, as the platinum—cage distance is increased then the cage—metal overlaps decrease in magnitude and the displacement of the metal in a "slip" distortion causes a smaller change in the metal—cage overlap integrals, since for the larger displacement the changes in the angular components to the overlap integrals change less.

In practice, for the pentagonal bipyramidal polyhedron the contraction in the B—B bond lengths vis à vis the icosahedron is accompanied by a displacement of the metal atom away from the cage face. Therefore the two effects discussed in the previous paragraph approximately cancel each other and the observed potential energy surface closely resembles that shown in Fig. 4b (curve 1b).

Conclusion

The calculations described above have reproduced very well differences in the structural parameters associated with pentagonal bipyramidal and icosahedral carbaplatinaboranes. In particular in constancy in Pt—B and Pt—C bond lengths in related 1,2,4-cage compounds have been related to the similar characteristics of the frontier orbitals of the pentagonal bipyramidal and icosahedral ligand fragments. The shorter equatorial ligand interatomic distances in the pentagonal bipyramidal clusters have been explained in terms of differences in bonding in the parent ligands. The larger "slip" distortion in the pentagonal bipyramidal 1,2,3- derivative has been shown in large measure to be due to the effect of the elevation angle of the substituents in the open faces of the ligands.

Acknowledgements

We thank the Gulbenkian Foundation and the S.R.C. for financial support.

References

1 M.F. Hawthorne, J. Organometal. Chem., 100 (1975) 97.
2 R.M. Wing, J. Amer. Chem. Soc., 92 (1970) 1187.
3 L.F. Warren, Jr. and M.F. Hawthorne, J. Amer. Chem. Soc., 90 (1968) 4823.
4 K. Wade, J. Chem. Soc. Chem. Commun., (1971) 792.
5 P.A. Wegner, Inorg. Chem., 14 (1975) 212.
6 G. Glidewell, J. Organometal. Chem., 102 (1975) 339.
7 D.M.P. Mingos and M.I. Forsyth, J. Organometal. Chem., 146 (1978) C37.
8 W.E. Carroll, M. Green, F.G.A. Stone and A.J. Welch, J. Chem. Soc. Dalton, (1975) 2263.
9 A.J. Welch, J. Chem. Soc. Dalton, (1975) 1473.
10 D.M.P. Mingos, M.I. Forsyth and A.J. Welch, J. Chem. Soc. Chem. Commun., (1977) 605.
11 D.M.P. Mingos, J. Chem. Soc. Dalton, (1977) 602.
12 D.M.P. Mingos, M.I. Forsyth and A.J. Welch, J. Chem. Soc. Dalton, (1978) 1363.
13 G.K. Barker, M. Green, F.G.A. Stone and A.J. Welch, J. Chem. Soc. Dalton, (1980) 1186.
14 R. Hoffmann, Science, 211 (1981) 995.
15 H. Basch and H.B. Gray, Theor. Chem. Acta, 4 (1966) 367.
16 R. Hoffmann and W.N. Lipscomb, J. Chem. Phys., 37 (1962) 3179; 37 (1962) 2872.
17 F.A. Cotton and C.B. Harris, Inorg. Chem., 6 (1967) 367.
18 R. Hoffmann, J. Chem. Phys., 39 (1963) 1397.